Electronic Supplementary Information (ESI) for

Photocontrol of dynein motor activities by photoswitchable ATP antagonists

Sampreeth Thayyil,[a,b,#1] Yukinori Nishigami,[a,b,#1] Md. Jahirul Islam,[a,b,#2] P.K. Hashim,[a,b] Ken'ya Furuta,[c] Kazuhiro Oiwa,[c] Jian Yu,[d] Min Yao,[d] Toshiyuki Nakagaki [a,b], Nobuyuki Tamaoki[a,b]*

a. *Research Institute for Electronic Science, Hokkaido University, Kita 20, Nishi 10, Kita-Ku, Sapporo, Hokkaido, 001-0020, Japan*

b. *Graduate School of Life Science, Hokkaido University, Kita 10, Nishi 8, Kita-ku, Sapporo, Hokkaido, Japan, 060-0810*

c. *Advanced ICT Research Institute, National Institute of Information and Communications Technology, Kobe, Hyogo, 651-2492, Japan.*

d. *Faculty of Advanced Life Science, Hokkaido University, North10, West 8, Kita-ku, Sapporo, Hokkaido, 060-0810, Japan*

#1. *These authors contributed equally to this work.*

#2. *Current Address: Institute of Science and Technology Austria, A-3400 Klosterneuburg, Austria*

Correspondence should be addressed to N. T. (E-mail: tamaoki@es.hokudai.ac.jp)

Table of contents

1. Experimental

Chemicals

All chemicals and biochemical reagents were purchased from commercial sources (Merck, Wako Pure Chemical industries, Tokyo Chemical industries, Kanto Chemicals, Thermo Fisher Scientific) and used without further purification.

Instrumentation

JEOL (ECX-400) spectrophotometer was used to measure NMR spectra (^{1}H, ^{13}C, ^{31}P). Purity analysis of the synthesized Azo-Amide-PCP and Azo-Propyl-PCP molecules were performed by using the Shimadzu reversed-phase (RP) HPLC system. Freeze drying of the compounds was done by using an EYELA FDU-2200 lyophilization system. High-resolution mass spectroscopy analysis was performed by Thermo Scientific Exactive mass spectrometer with electron spray ionization (ESI). Chromatographic purification was performed using silica gel 60 N (neutral, 6-120 µm, Kanto chemicals). Absorption spectra were recorded by Shimadzu UV-1800 spectrophotometer. Thin-layer chromatography was performed on precoated silica gel 60 F_{254} aluminum sheets (MERCK). Asahi Spectra CL-1503 LED controller and Hamamatsu LED controller were used for 430 nm and 365 nm light for photoisomerization studies and reversible modulation of the activities of dynein in *in vitro* motility assay.

2. Synthesis

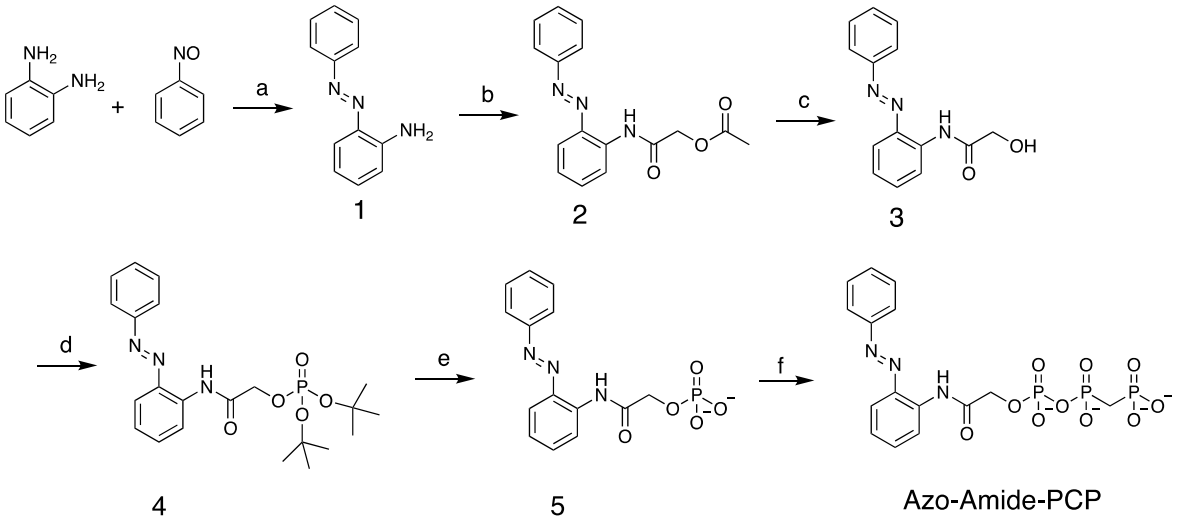

Reagent and condition: (a) AcOH, toluene, N_2, 60 °C, 24 h; (b) Acetoxyacetyl chloride, Triethylamine, DCM, r.t, 1 h.; (c) K_2CO_3, MeOH, RT, overnight; (d) di-*tert*-butyl *N*,*N*-diisopropylphosphoramidite, 1*H*-tetrazole, dry THF, Ar, r.t, 7 h; then, mCPBA, 0 °C, 1h; then rt, 40 min; (e) trifluoroacetic acid, dry CH_2Cl_2, Ar, r.t, 6 h; then eluting through DEAE Sephadex A-25 anion exchanger, TEAB; (f) tributylamine, carbonyldiimidazole, tributylammonium, methylenediphosphate, dry DMF, Ar, rt, overnight.

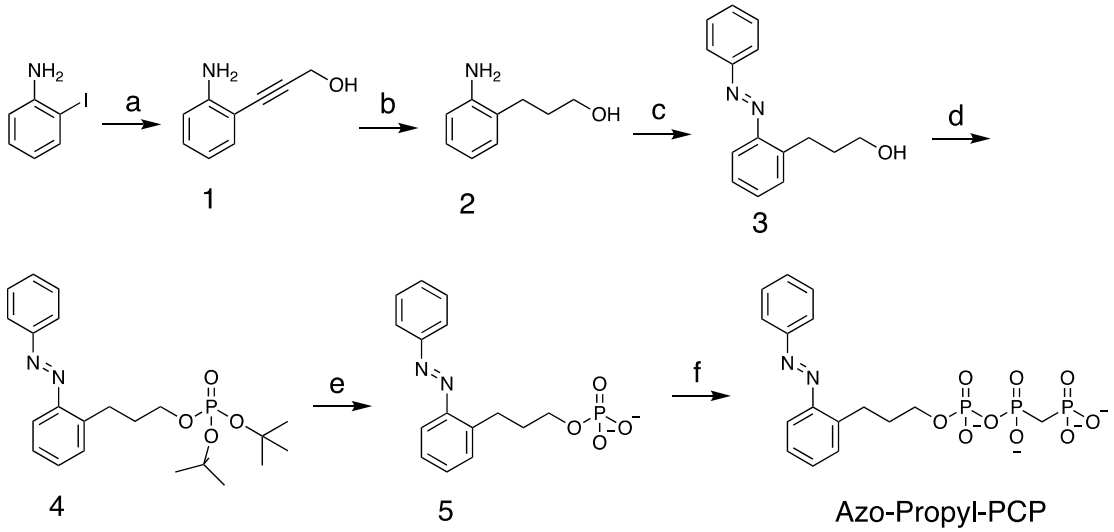

Reagent and condition: (a) CuI, bis(triphenylphosphine)palladium(II) dichloride, 2-propyn-1-ol, triethylamine, r.t, 18 h; (b) 10% Pd/C, H_2, MeOH, RT, 48 h; (c) Nitrosobenzene, AcOH, toluene, N_2, 60 °C, 21 h; (d) Di-tert-butyl N,N-diisopropylphosphoramidite, 1H-tetrazole, dry THF, Ar, r.t, 6 h, then mCPBA, 0 °C, 1 h; (e) TFA, dry DCM, Ar, RT, 6 h; (f) Tributylamine, carbonyldiimidazole, tributylammonium methylenediphosphonate, dry DMF, Ar atmosphere, r.t, overnight.

General synthetic procedure for the monophosphate into triphosphate conversion

First, a solution of methylenediphosphonic acid (6.5 eq) in (2 ml) of water was added dropwise to a flask containing tributylamine (2 eq) at 4 °C with vigorous shaking. The solvent was evaporated at 30 °C room temperature with dry-MeOH (3 x 30 mL) to prepare tributyl ammonium methylenediphosphonate and dried under vacuum.

Then, tributyl ammonium salt of compound **5** was prepared by mixing compound **5** in dry MeOH with tributylamine (3.3 eq) followed by the solvent evaporation. The crude mixture obtained was dissolved in dry DMF and added a solution of 1,1'- carbonyldiimidazole (6.3 eq) in dry DMF under Ar at room temperature. After 16 h, dry MeOH (0.2 eq) was added and stirred for another 1 h to quench the excess 1,1'- carbonyldiimidazole. Then, the reaction mixture was added dropwise to a dry DMF solution of above prepared tributyl ammonium methylenediphosphonate. After 12 h, the reaction mixture was cooled to 0 °C in an ice bath, added cold water and pH adjusted to 7.5 using 1 M NaOH. Diethyl ether was added to the reaction mixture, the compound extracted in water and the aqueous phase was evaporated with EtOH at 30°C and dried under vacuum. The residue was dissolved in 0.2 M triethyl-ammonium hydrogen carbonate (TEAB), applied to DEAE-Sephadex A-25 column (2.5x 30 cm, 10 g), and eluted with a linear gradient (0.2M-1.0M; total volume; 1L) of TEAB solution (over 400 min) at 4 °C. The target elution fraction was collected and evaporated with EtOH at 30°C several times to remove TEAB buffer and dried under vacuum. The obtained residue was redissolved in dry MeOH (2 ml). Then, a 1 M NaI in acetone (5 ml) was added to above mixture where the sodium salt of the target compound precipitated. The precipitate was filtered and washed with acetone several times followed by lyophilization.

Azo-Amide-PCP (Yield. 65%): ^{1}H NMR (400 MHz, D_2O) δ 8.01 – 7.94 (m, 3H), 7.73 (d, *J* = 8.1, 1H), 7.66 – 7.60 (m, 4H), 7.43 (t, *J* = 7.4 Hz, 1H), 4.67 (d, *J* = 7.3 Hz, 2H), 2.35 (t, *J* = 20.4 Hz 2H), ^{13}C NMR (100 MHz, D_2O, CD_3OD as the standard) δ 171.36 (d, *J* = 9.3 Hz), 153.14 (s), 144.27 (s), 134.92 (s), 133.54 (s), 133.08 (s), 130.64 (s), 127.69 (s), 124.99 (s), 123.85 (s), 118.14 (s), 65.63 (s), 28.90 (d, *J* = 5.6 Hz).). ^{31}P NMR (160 MHz, D_2O (H_3PO_4) as the external standard) δ 15.69 (d, *J* = 8.6 Hz), 8.42 (dd, *J* = 25.9, 8.6 Hz), -11.94 (d, *J* = 25.9 Hz). HR-MS (ESI, m/z) calculated for $C_{15}H_{15}N_3Na_4O_{10}P_3$ $[M+H]^+$: 581.95556; found: 581.95581.

Azo-Propyl-PCP (yield 61%): ^{1}H NMR (400 MHz, D_2O) δ 7.94 (dd, J = 8.0, 1.8 Hz, 2H), 7.66–7.48 (m, 6H), 7.42-7.38 (m, 1H), 3.99 (q, J = 6.6 Hz, 2H), 3.20 (t, J = 7.9 Hz, 2H), 2.28 (t, J = 20.6 Hz, 2H), 1.97 (quin, J = 7.9 Hz, 2H). ^{13}C NMR (100 MHz, D_2O, CD_3OD as the standard) δ 153.31 (s), 151.44 (s), 141.84 (s), 132.67 (d, *J* = 7.8 Hz), 132.03 (s), 130.58 (s), 128.22 (s), 123.59 (s), 116.75 (s), 66.86 (d, *J* = 5.9 Hz), 33.18 (d, *J* = 7.5 Hz), 30.32 (d, *J* = 7.0 Hz), 28.19 (s). ^{31}P NMR (160 MHz, D_2O (H_3PO_4) as the external

standard) δp 14.64 (d, *J* = 8.3 Hz), 8.32 (dd, *J* = 25.7, 7.9 Hz), -10.54 (d, *J* = 25.7 Hz). HR-MS (ESI, m/z) calculated for $C_{16}H_{18}N_2Na_4O_9P_3$ $[M+H]^+$: 566.98104; found: 566.98235.

3. Purity analysis of Azo-Amide-PCP and Azo-Propyl-PCP by reverse-phase HPLC

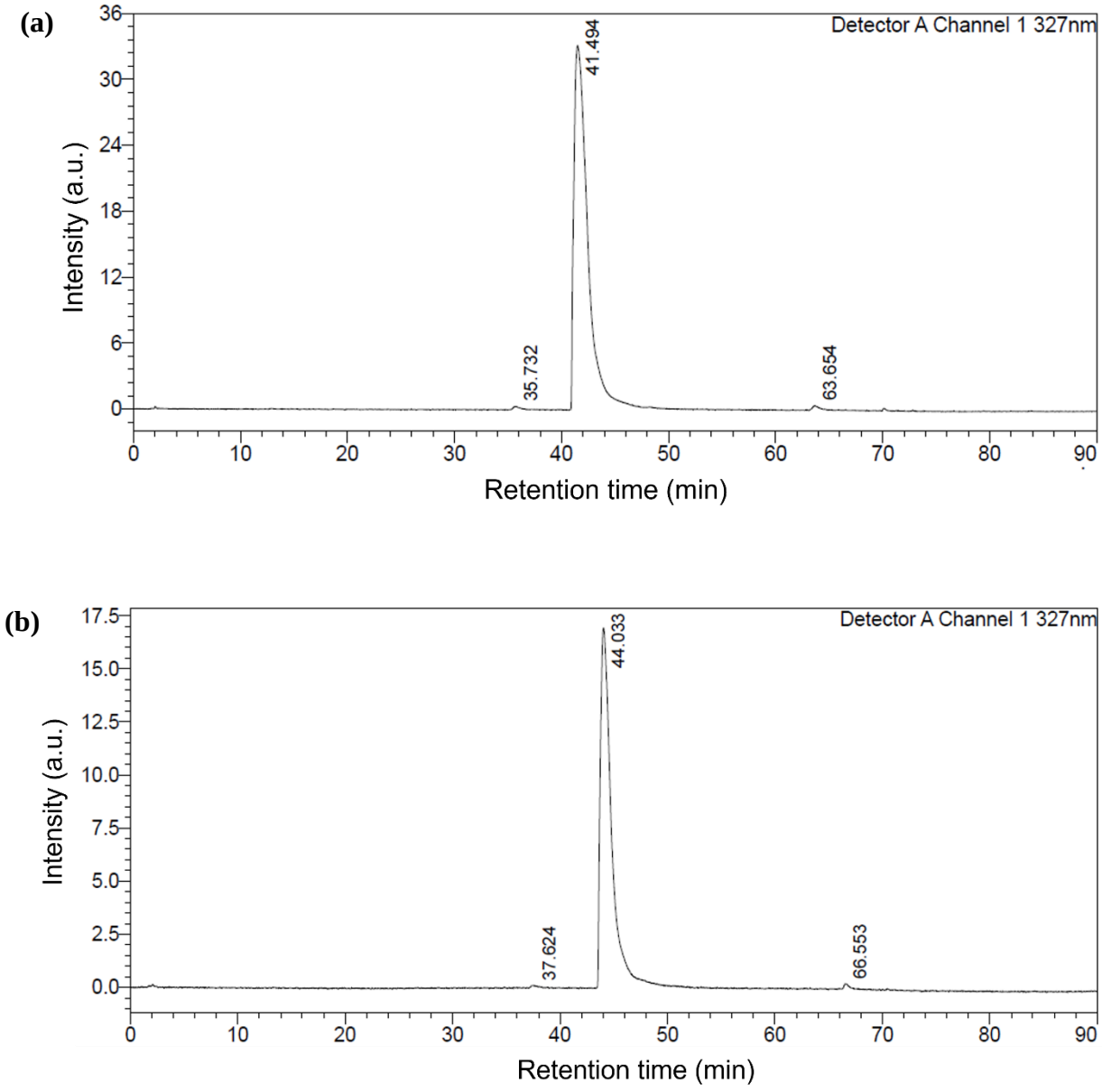

Fig. S1 Reverse phase HPLC chromatograms (detection wavelength 327 nm, flow rate: 1.0 mL/min, room temperature) of **Azo-Amide-PCP** (a) and **Azo-Propyl-PCP** (b) that show > 96 % purity. 10–70 % of CH_3CN in sodium phosphate buffer (pH 6) used as eluent with Mightysil column (RP-18 GP (L) 150 x 4.6, 5µm, Kanto Chemical).

4. ^{1}H-NMR analysis of *cis*/*trans* isomer ratio at the UV_{PSS} (365 nm) and Vis_{PSS} (430 nm)

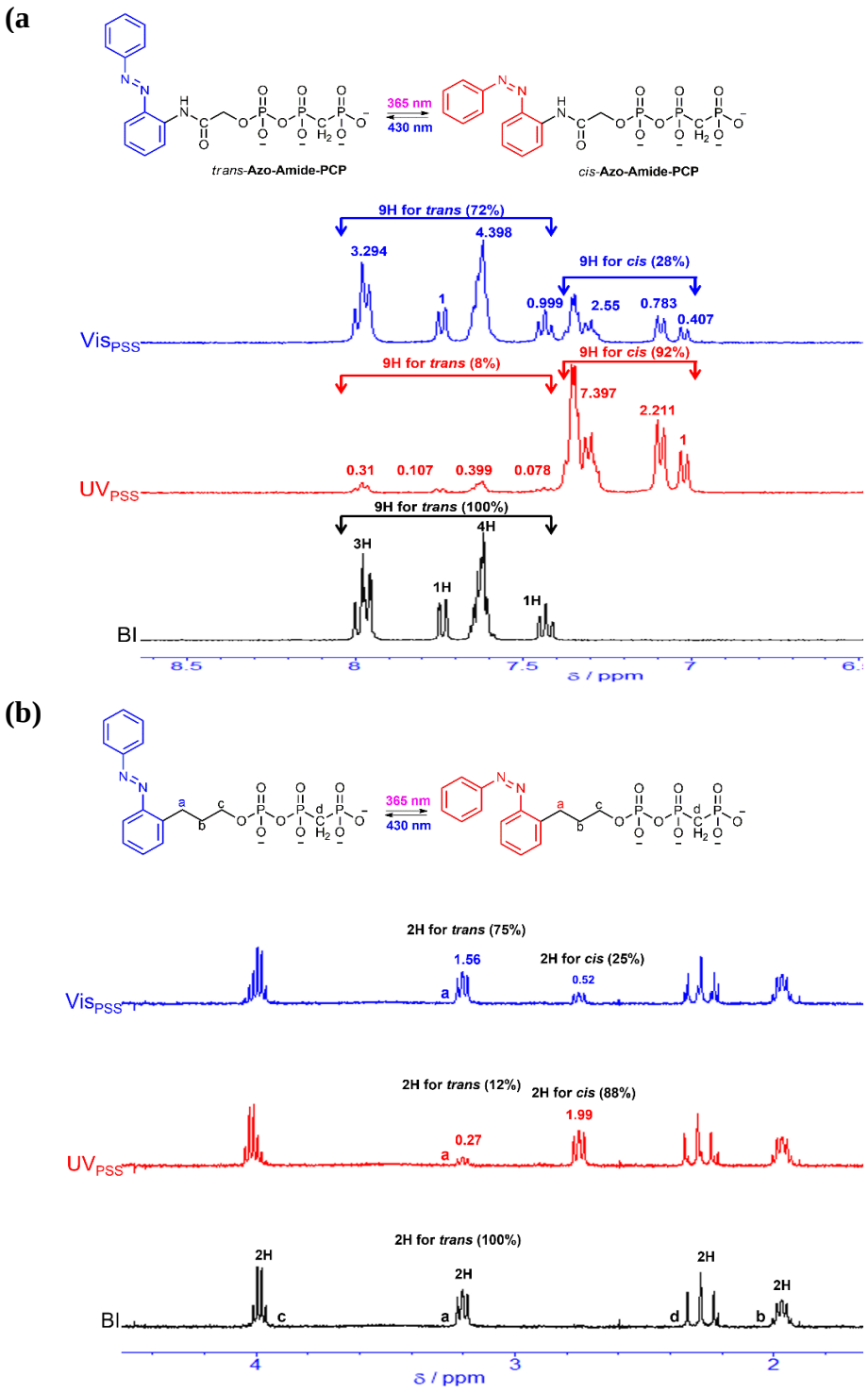

Fig. S2 ^{1}H NMR (400 MHz, D_2O) showing the *cis*/*trans* isomer ratios of (a) Azo-Amide-PCP, (b) Azo-Propyl-PCP at before irradiation (BI), UV_{PSS} (365nm) and Vis_{PSS} (430nm).

5. Isomer ratio of *trans* and *cis* isomer at UV_{PSS} (365 nm) and Vis_{PSS} (430 nm)

Table S1. *cis/trans* ratio of photoresponsive ATP antagonists.

ATP antagonists	UV_{PSS}		Vis_{PSS}	
	cis	*trans*	*cis*	*trans*
AzoTP[1]	92%	8%	29%	71%
Azo-Amide-PCP	92%	8%	28%	72%
Azo-Propyl-PCP	88%	12%	25%	75%

6. Thermal stability of *cis* isomers of Azo-Amide-PCP and Azo-Propyl-PCP

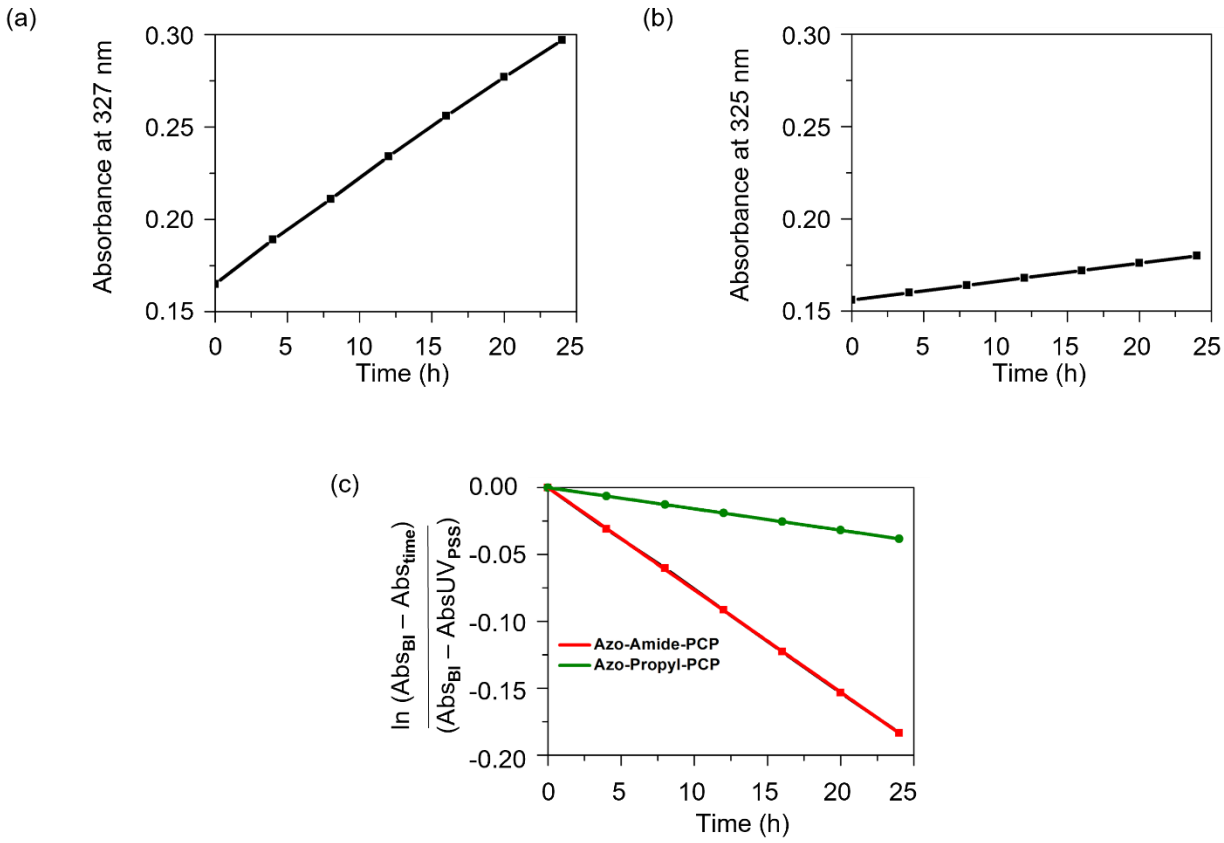

Fig. S3 Time course absorbance changes due to thermal back *cis–trans* isomerization of Azo-Amide-PCP (5.93 x 10^{-4} M) (a), Azo-Propyl-PCP (4.73 x 10^{-4} M) (b) in BRB-80 buffer (pH 6.9) after UV_{PSS} at 25°C. The plot showing the rate of thermal back isomerization calculated using the equation, $\ln\left(\frac{(Abs\ (BI) - Abs\ (time)}{Abs(BI) - Abs(UVPSS)}\right) = -kt$, Absorbances at before irradiation (Abs (BI)), at UV photostationary state (Abs (UV_{PSS}), at different time interval (Abs (time)) (c). Rate constant k = 0.0076 h^{-1} ($t_{1/2}$ = 91 h) for Azo-Amide-PCP and k = 0.0016 h^{-1} ($t_{1/2}$ = 430 h) for Azo-Propyl-PCP.

7. *In vitro* microtubule-dynein motility assay in the presence AzoTP

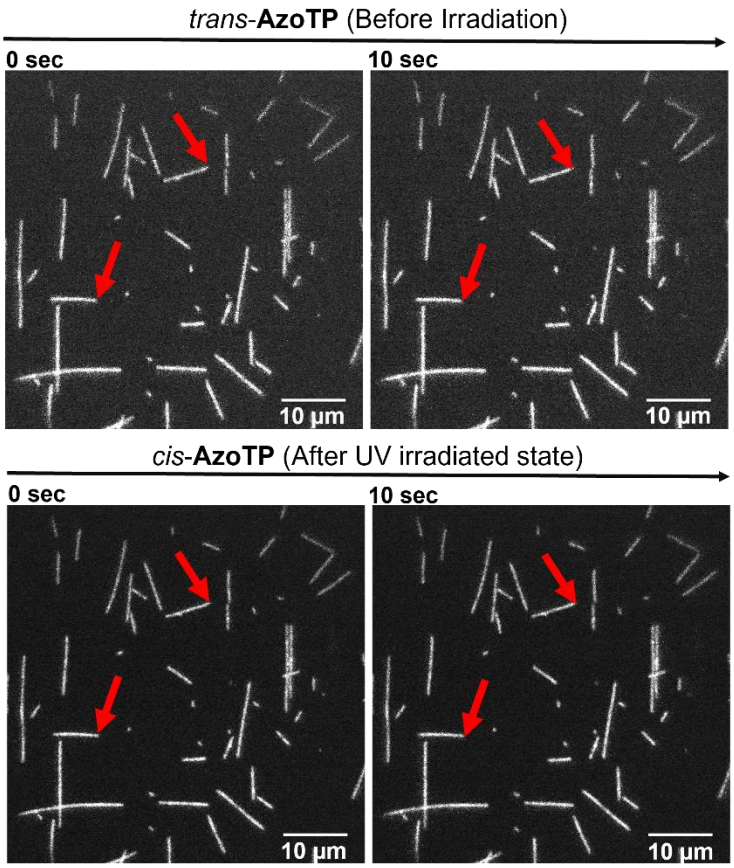

Fig. S4 Fluorescence microscopy images of the microtubules obtained at 0 s and 10 s before and after UV irradiation to the flow cell containing AzoTP (1.0 mM). Red arrow indicates the position of the same microtubule at 0 s and 10 s with no significant changes.

8. Phosphate standard curve and basal ATPase of human cytoplasmic dynein construct

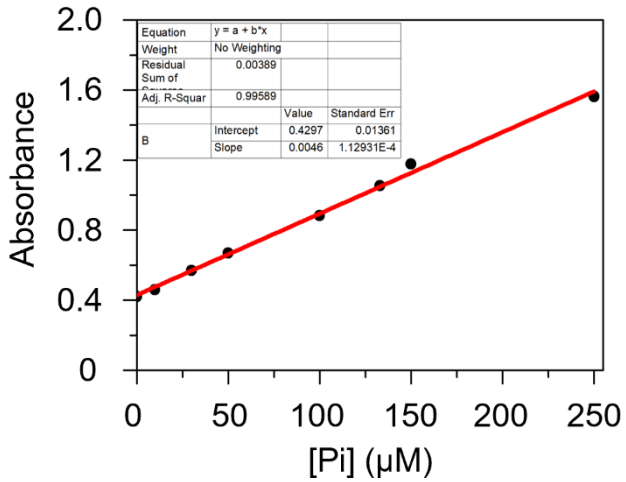

Fig. S5 Phosphate calibration curve used for the calculation of ATP and AzoTP hydrolysis assay.

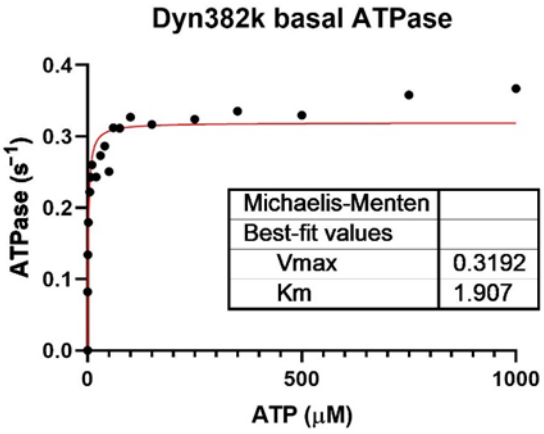

Fig. S6 Cytoplasmic dynein ATPase in the absence of microtubules. The ATPase data are replotted from Ibusuki et al. (reference 30 of main text)[4] to clarify the scatter of data points and the goodness of fitting.

9.Control experiments of *Chlamydomonas* with UV and Vis light irradiation

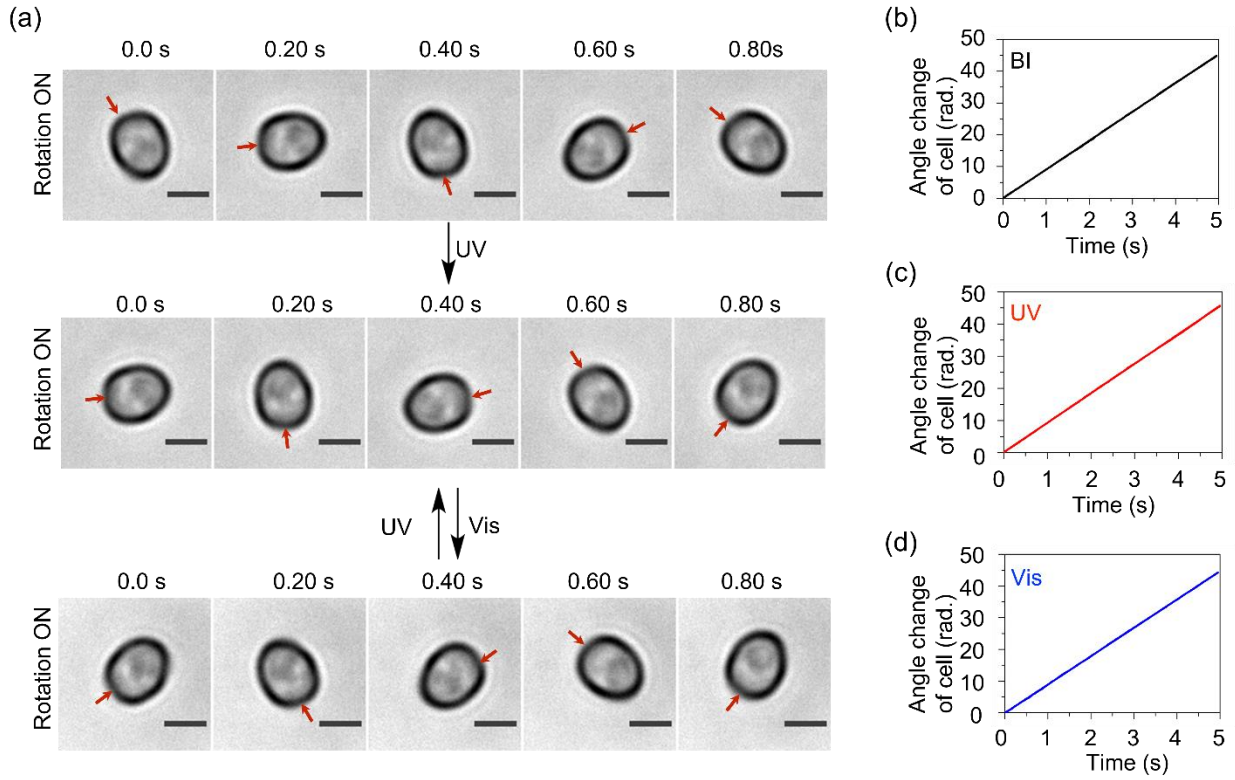

Fig. S7 Optical microscopy images of the *Chlamydomonas reinhardtii* cell at time 0–0.8 s before and after UV (5 s)/Vis (7 s) light irradiations to the flow cell containing ATP (100 μM) without ATP antagonists (a). Scale bars: 5 μm. Red arrows head indicate the reference point of the cell rotation. Graph showing the angle change of *Chlamydomonas* cell at time 0–5 s before (b) and UV (c)/Vis (d) light irradiations. Repeated UV/Vis light irradiation without ATP antagonists showed no significant effect on the rotational motion *Chlamydomonas* cell. The rate of angle change was 9.10 rad. s^{-1} (BI), 9.18 rad. s^{-1} (UV_{PSS}) and 8.95 rad. s^{-1} (Vis_{PSS}).

10. Photoregulation of *Chlamydomonas* by Azo-Propyl-PCP

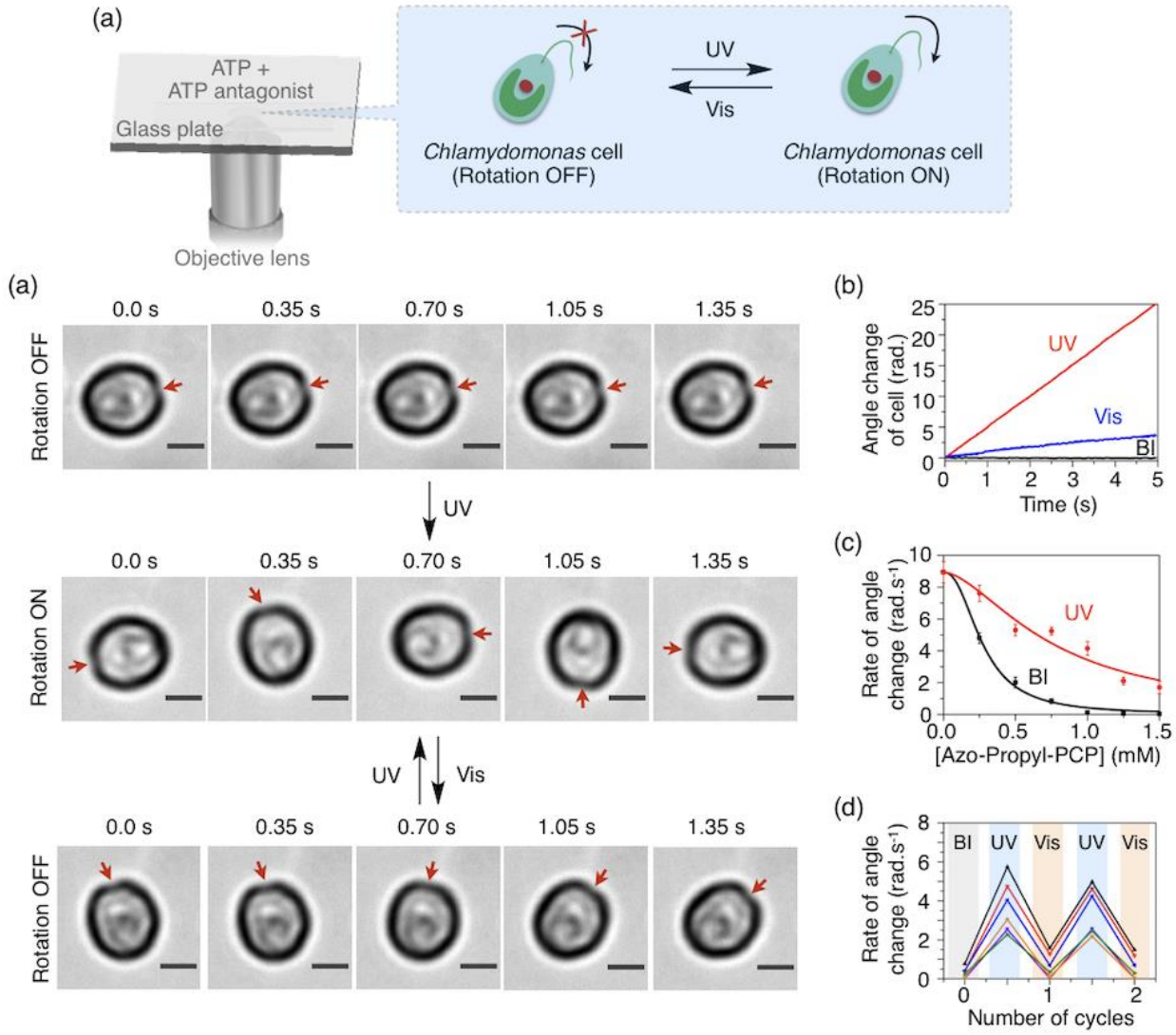

Fig. S8 Optical microscopy images showing the rotational motion of the *Chlamydomonas reinhardtii* cell at time 0–1.35 s before and after UV (5 s)/Vis (7 s) light irradiations to the flow cell containing Azo-Propyl-PCP (1.0 mM) and ATP (100 μM) (a). Scale bars: 5 μm. (red arrows head indicate the reference point of the cell rotation. Graph showing the rate of angle change of the cell with different concentrations of Azo-Propyl-PCP (K_m = 0.14 ± 0.04 mM).[2] (b), the angle change of *Chlamydomonas* cell at time 0–5 s (c), and the reversible switching in the rate of angle change of 6 different cells (black, red, blue, orange, purple and green lines) over 2 cycles before (BI) and after UV/Vis light irradiations (d). Error bars represent the standard error of 8–10 cells.

11. Normalized equation for fitting the *Chlamydomonas* experimental data

Based on the observation of the less-efficient inhibition effect at lower inhibitor concentration in the cell experiment, we set a cooperative inhibition model as shown by the following reaction for the analysis of *Chlamydomonas* rotational activity at different concentration of ATP antagonists.

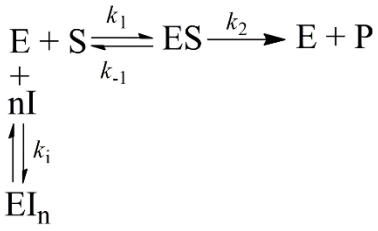

where E, S, I, P, and n are dynein, ATP, ATP antagonists as inhibitors, ADP with phosphate, and the number of inhibitors attaching the dynein. The rate constants of each reaction are k_1, k_{-1}, and k_2. The dissociation constant between dynein and ATP becomes $K_\mathrm{m} = [\mathrm{E_0}][\mathrm{S_0}]/[\mathrm{ES_0}]$, and the total concentration of dynein is $[\mathrm{E_{t0}}] = [\mathrm{E_0}] + [\mathrm{ES_0}]$, in which subscript 0 means the absence of ATP antagonists. Using these equations, the concentration of the dynein-ATP complex becomes $[\mathrm{ES_0}] = [\mathrm{E_{t0}}][\mathrm{S_0}]/(K_\mathrm{m} + [\mathrm{S_0}])$. Then, in the presence of the inhibitor, the dissociation constant for dynein and ATP is $K_\mathrm{m} = [\mathrm{E}][\mathrm{S}]/[\mathrm{ES}]$, and the dissociation constant for dynein and inhibitor is $K_\mathrm{i} = [\mathrm{E}][\mathrm{I}]^n/[\mathrm{EI}_n]$. In this condition, the total amount of enzymes is $[\mathrm{E_t}] = [\mathrm{E}] + [\mathrm{EI}_n] + [\mathrm{ES}]$. Using these equations, the concentration of the dynein-ATP complex becomes $[\mathrm{ES}] = [\mathrm{E_t}][\mathrm{S}]/([\mathrm{S}] + (1 + [\mathrm{I}]^n/K_\mathrm{i})K_\mathrm{m})$. When the reaction rates in the presence and absence of ATP antagonists are expressed as $v_\mathrm{i} = k_2[\mathrm{ES}]$ and $v_0 = k_2[\mathrm{ES_0}]$, respectively, their ratio becomes $v_\mathrm{i}/v_0 = [\mathrm{ES}]/[\mathrm{ES_0}]$. In this experiment, the dynein concentration is constant regardless of the presence or absence of ATP antagonists. The amount of free ATP is also considered almost constant under these conditions to be regarded as $[\mathrm{E_t}] = [\mathrm{E_{t0}}]$ and $[\mathrm{S}] = [\mathrm{S_0}]$. Therefore, the rate of dynein activity will be $v_\mathrm{i} = v_0\,(K_\mathrm{m} + [\mathrm{S}])/([\mathrm{S}] + (1 + [\mathrm{I}]^n/K_\mathrm{i})K_\mathrm{m})$. In our analysis, we used this equation to evaluate the angle change of the demembranated *Chlamydomonas*. The n represents the cooperativity of ATP analogs for dynein, and higher the value means higher the cooperativity. By fitting the experimental data to the equation, n of Azo-Amide-PCP were 2.4 (*trans*) and 3.6 (*cis*) while those of Azo-Propyl-PCP was 2.3 (*trans*) and 1.67 (*cis*). The cooperativity of Azo-Amide-PCP for binding to dynein is higher in the *cis*-isomer. In comparison, the cooperativity of Azo-Propyl-PCP is higher in the *trans* isomer.

12. Molecular docking

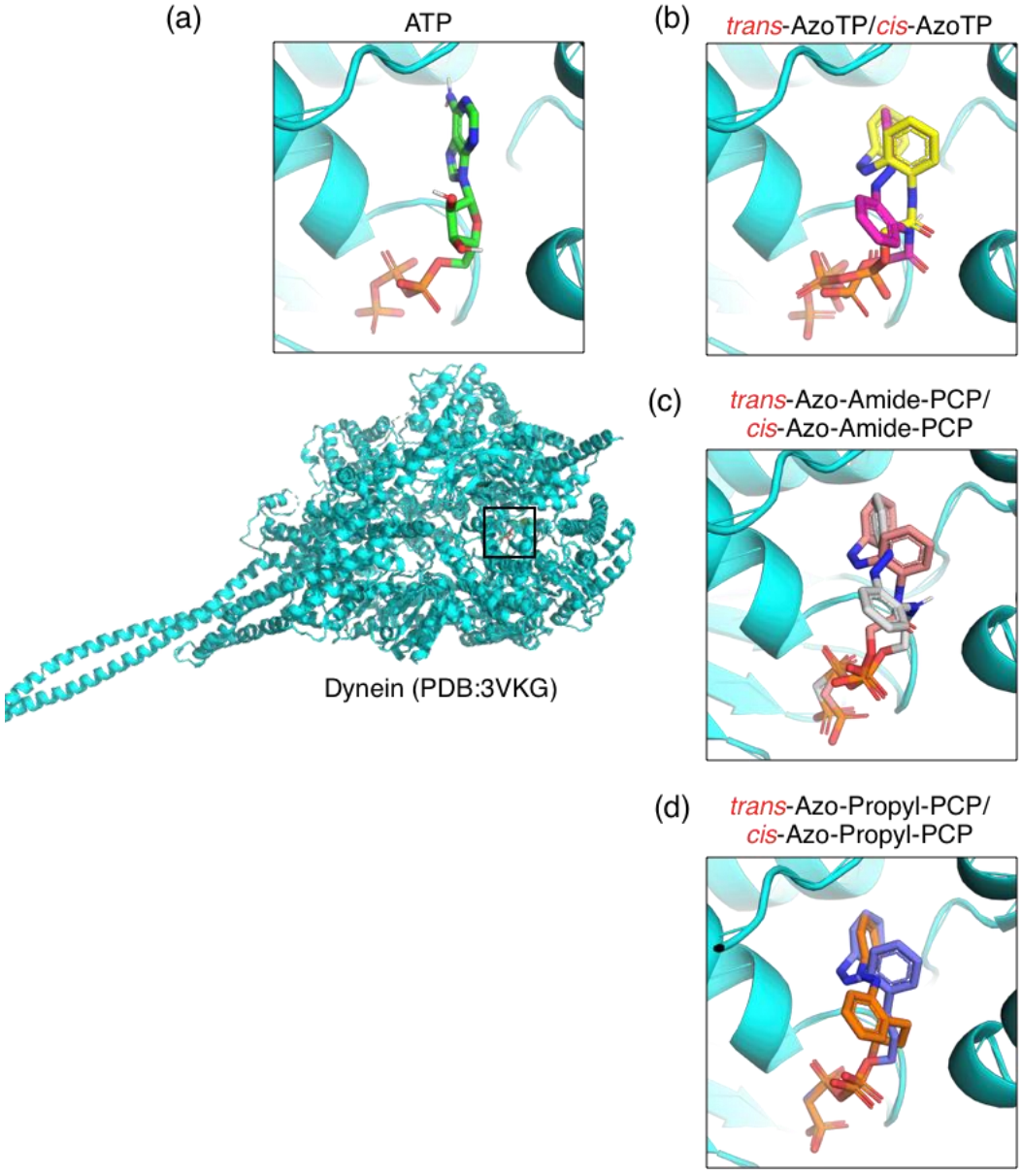

Fig. S9 Scheme showing the docked ligands in the ATP binding site of cytoplasmic dynein (AAA1 chain; PDB 3VKG) (a). The superimposed docked ligands in the binding site of dynein AAA1 chain *trans*/*cis*-AzoTP (b), *trans*/*cis*-Azo-Amide-PCP (c) and *trans*/*cis*-Azo-Propyl-PCP (d).

13. NMR spectral data.

^{1}H NMR ^{13}C NMR and ^{31}P spectra of Azo-Amide-PCP

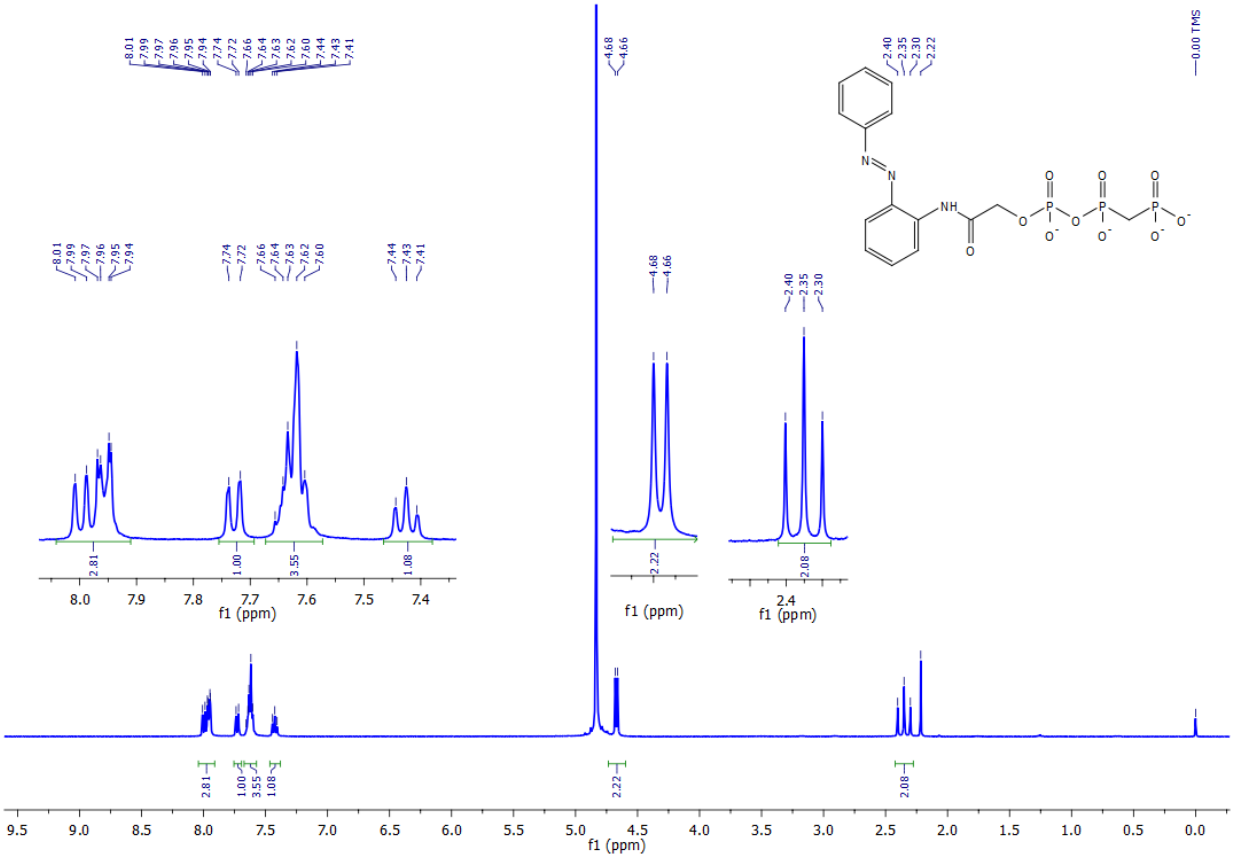

Fig. S10 ^{1}H NMR of Azo-Amide-PCP

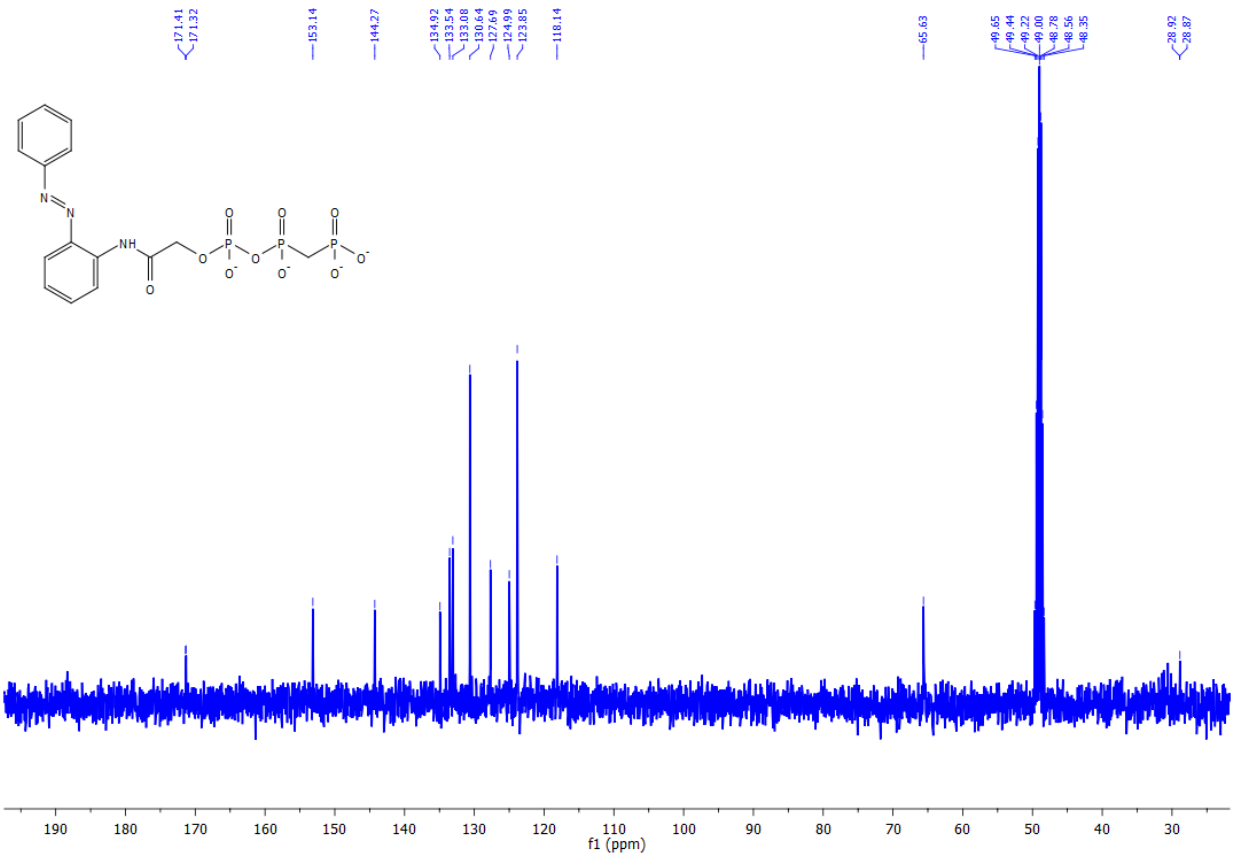

Fig. S11 ^{13}C NMR of Azo-Amide-PCP

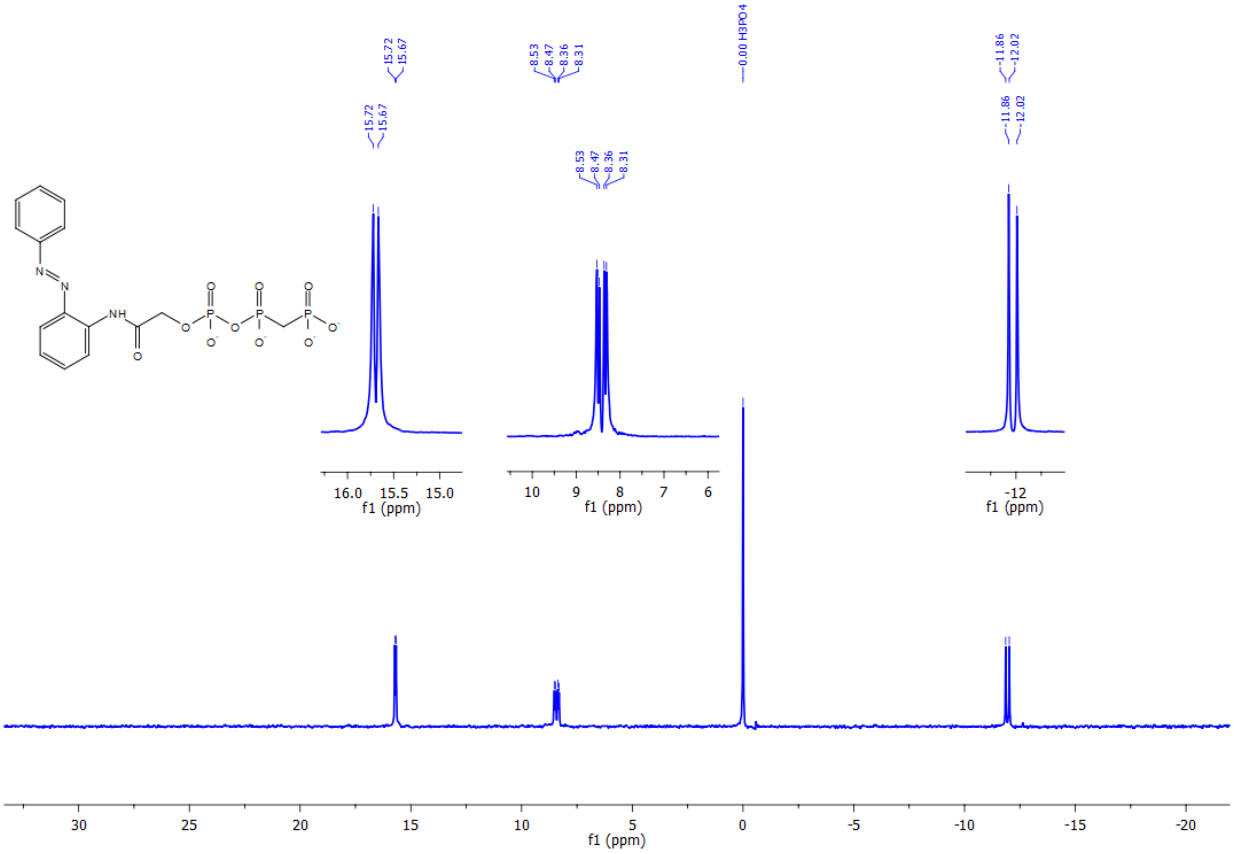

Fig. S12 ^{31}P NMR of Azo-Amide-PCP

^{1}H NMR ^{13}C NMR and ^{31}P spectra of Azo-Propyl-PCP

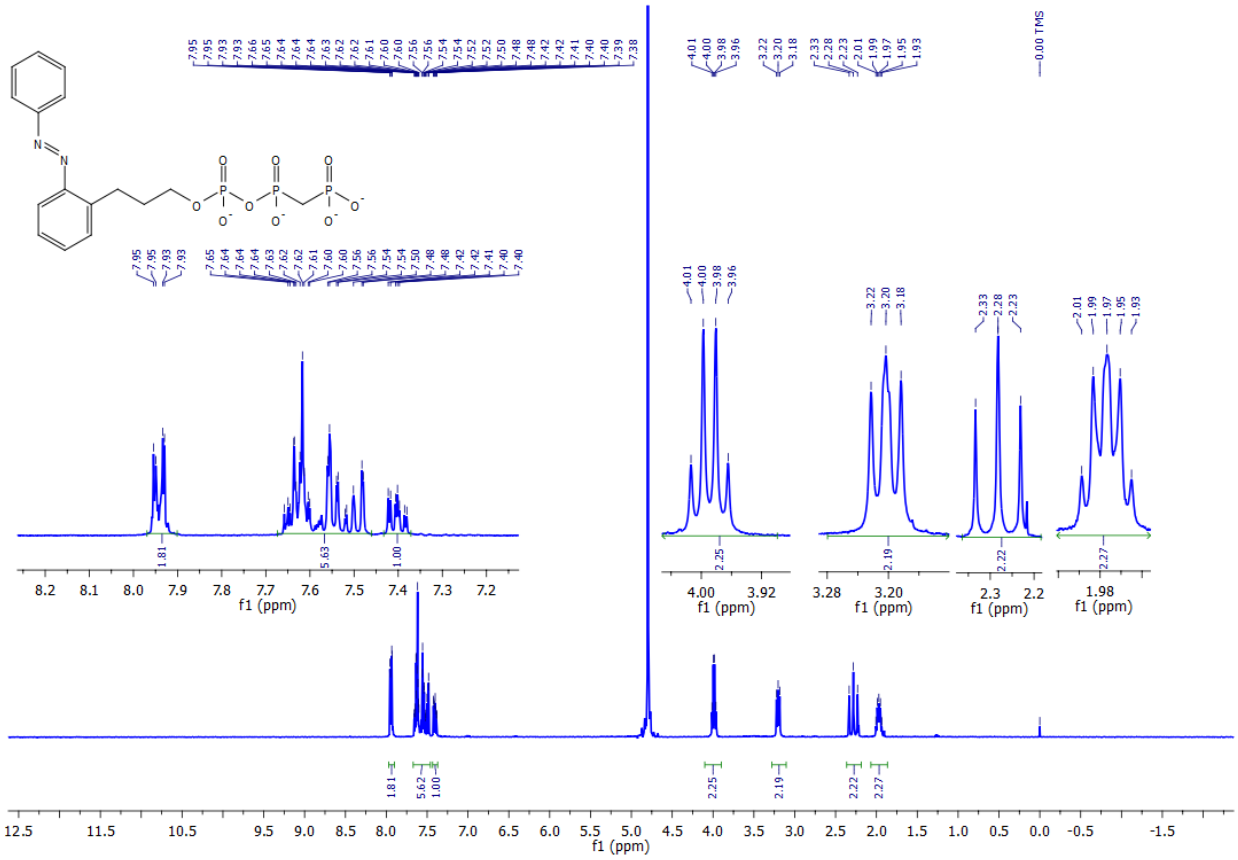

Fig. S13 ^{1}H NMR of Azo-Propyl-PCP

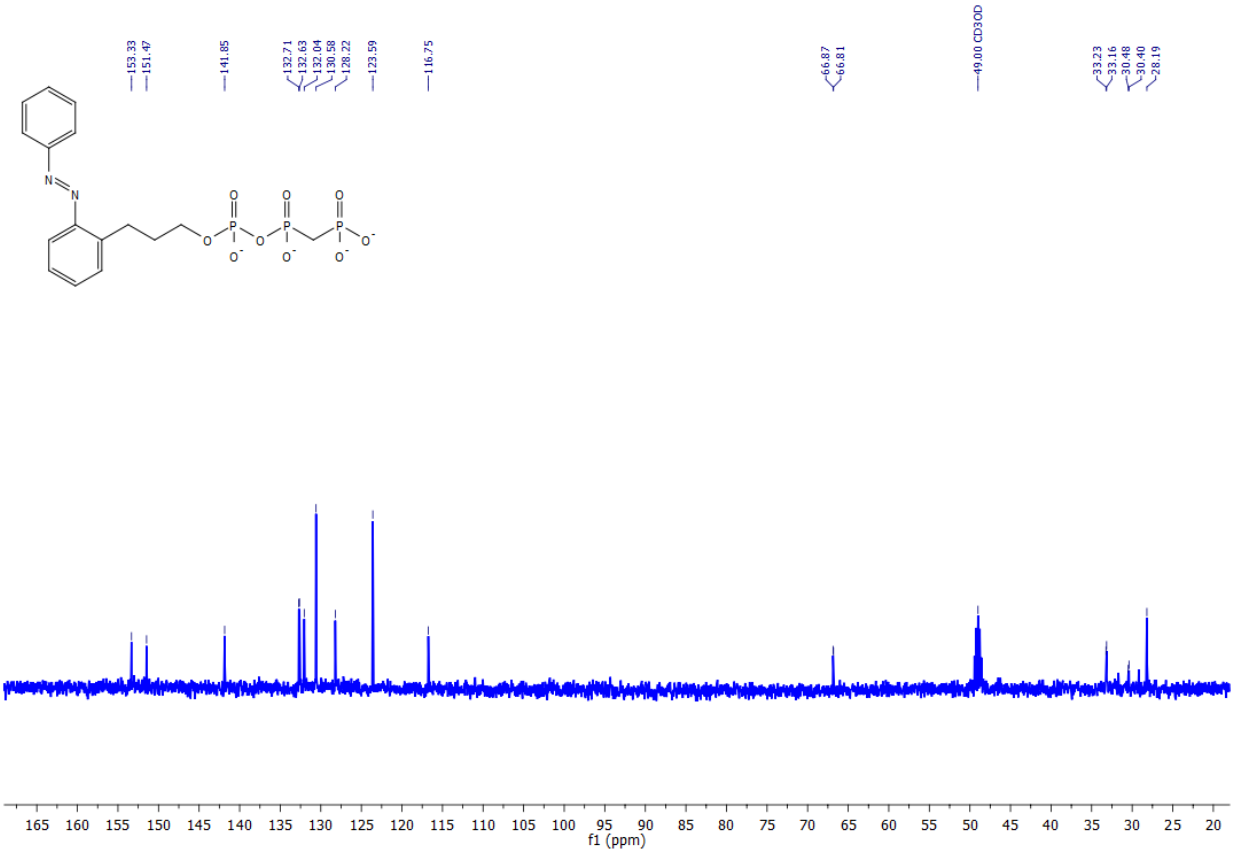

Fig. S14 ^{13}C NMR of Azo-Propyl-PCP

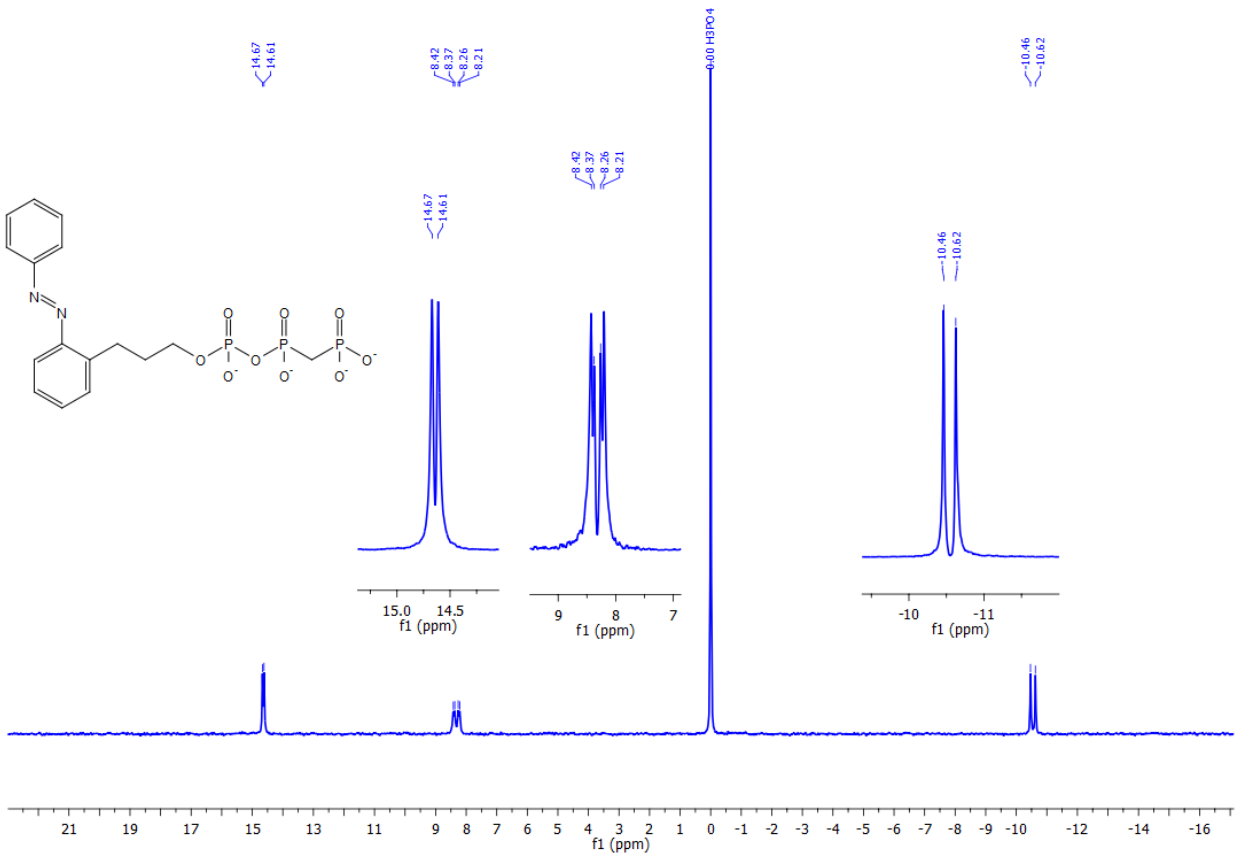

Fig. S15 ^{31}P NMR of Azo-Propyl-PCP

14. High resolution mass spectra of Azo-Amide-PCP and Azo-Propyl-PCP

(a)

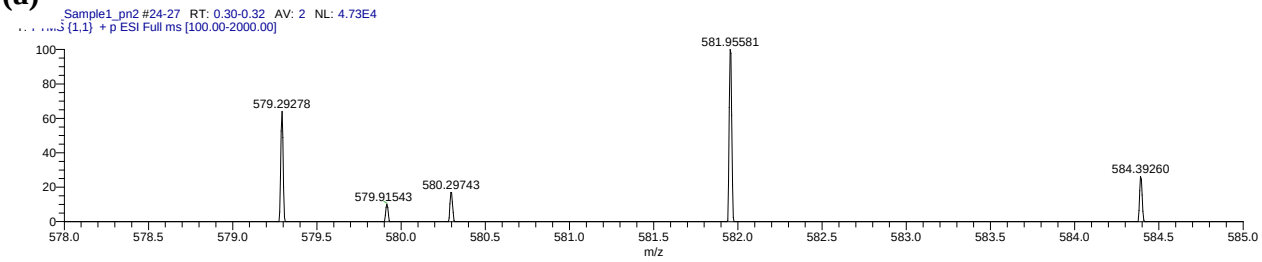

Azo-Amide-PCP. Calculated for $C_{15}H_{15}N_3Na_4O_{10}P_3$ [M-H] $^+$: 581.95556; found: 581.95581.

(b)

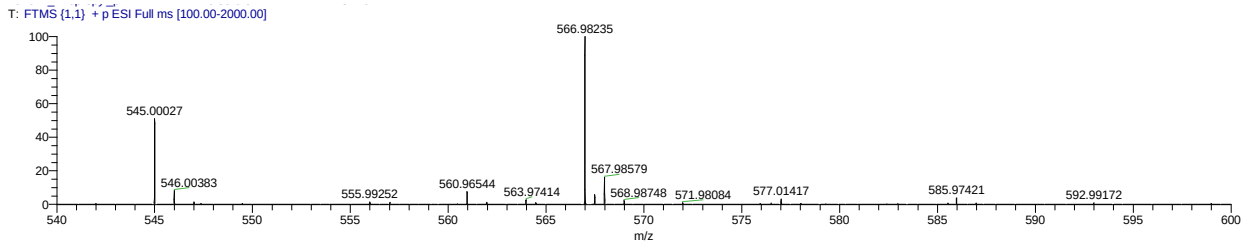

Azo-Propyl-PCP. Calculated for $C_{16}H_{18}N_2Na_4O_9P_3$ [M-H] $^+$: 566.98104; found: 566.98235.

Fig. S16 High-resolution mass spectra

15. Supplementary movies information.

Movie S1: Movie (total 3 min, 30fps, 3x faster) showing the inhibition of microtubule motion in the presence of AzoTP (1 mM, *trans*) in a microtubule-dynein i*n vitro* motility assay system.

Movie S2: Movie demonstrating the inhibition of microtubule motion and reversible photocontrol of cytoplasmic dynein in *in vitro* motility assay using AzoTP (5 mM) in the presence of 100 μM ATP (total 3 min, 30fps, 3x faster). Before irradiation the microtubule filaments were moving very slowly (inhibited), however moved faster after shining UV light, which was again inhibited by Vis light irradiation.

Movie S3: Movie demonstrating the inhibition of microtubule motion and reversible photocontrol of cytoplasmic dynein in *in vitro* motility assay using Azo-Amide-PCP (5 mM) in the presence of 50 μM ATP (total 4 min, 30fps, 3x faster). Before irradiation the microtubule filaments were moving very slowly (inhibited), however moved faster after shining UV light, which was again inhibited by Vis light irradiation.

Movie S4-A: Movie (total 1.8 min, 30fps, 1.5x faster) showing the reversible photoregulation of rotation of many *Chlamydomonas* cells by alternating illumination of 365 nm (5s) and 430 nm (7s) using Azo-Propyl-PCP (1 mM) in the presence of 100 μM ATP.

Movie S4: This movie (total 1.8 min, 30fps, 1.5x faster) demonstrates the photoresponsive modulation of the rotation of selected single cell *Chlamydomona*s with Azo-Propyl-PCP (1 mM) in the presence of 100 μM ATP.

Movie S5-A: Movie (total 1.8 min, 30fps, 1.5x faster) showing the photoregulation of rotation of many *Chlamydomonas* cells by alternating illumination of 365 nm (5s) and 430 nm (7s) using Azo-Amide-PCP (1.25 mM) in the presence of 100 μM ATP. The speed change from almost off to faster and then to slower could be seen by the illumination of UV and Vis light.

Movie S5: Movie (total 1.8 min, 30fps, 1.5x faster) show the photoresponsive modulation of the rotation of selected single cell *Chlamydomonas* with Azo-Amide-PCP (1.25 mM) in the presence of 100 μM ATP.

Movie S6: Movie (total 1.8 min, 30fps, 1.5x faster) demonstrates the repeated photoregulation of rotational speed changes of many *Chlamydomonas* cells by alternating illumination of 365 nm (5s) and 430 nm (7s) using Azo-Propyl-PCP (1 mM) in the presence of 100 μM ATP.

Movie S7: Movie (total 1.8 min, 30fps, 1.5x faster) demonstrates the repeated photoregulation of rotational speed changes of many *Chlamydomonas* cells by alternating illumination of 365 nm (5s) and 430 nm (7s) using Azo-Amide-PCP (1.25 mM) in the presence of 100 μM ATP.

16. References

1. N. Perur, M. Yahara, T. Kamei and N. Tamaoki, *Chem. Commun.*, 2013, **49**, 9935–9937.

2. T. Torisawa, M. Ichikawa, A. Furuta, K. Saito, K. Oiwa, H. Kojima, Y.Y. Toyoshima, K. Furuta. *Nat.Cell Biol*, 2014, **16**, 1118–1124

3. W. Takano, T. Hisabori and K. I. Wakabayashi, *J. Biol. Chem.*, 2021, **296**, 100156.

4. R. Ibusuki, T. Morishita, A. Furuta, S. Nakayama, M. Yoshio, H. Kojima, K. Oiwa, and K. Furuta. *Science*, **2022**, in press.